Sensors and Actuators B 134 (2008) 953–958

Contents lists available at ScienceDirect

Sensors and Actuators B: Chemical

journal homepage: www.elsevier.com/locate/snb

Demonstration of MEMS-based differential scanning calorimetry for determining thermodynamic properties of biomolecules

Li Wang[a], Bin Wang[b], Qiao Lin[b,*]

[a] Department of Mechanical Engineering, Carnegie Mellon University, Pittsburgh, PA 15213, United States
[b] Department of Mechanical Engineering, Columbia University, New York, NY 10027, United States

ARTICLE INFO

Article history:
Received 10 April 2008
Received in revised form 14 June 2008
Accepted 30 June 2008
Available online 22 July 2008

Keywords:
MEMS thermal sensor
Differential scanning calorimetry
Biomolecular thermodynamics
Biomolecular interactions
Protein conformational transitions

ABSTRACT

We demonstrate microelectromechanical system (MEMS)-based differential scanning calorimetry (DSC) for characterizing thermodynamic properties of biomolecules. The MEMS device consists of a pair of polydimethylsiloxane (PDMS) calorimetric microchambers and fluid handling microchannels, with each chamber 1.2 μl in volume and based on a freestanding SU-8 diaphragm. A nickel–chromium thermopile, and nickel heaters and temperature sensors, are integrated on the diaphragms to allow thermal measurement and control. During DSC measurements, the chambers are filled with a biomolecular solution and reference buffer, respectively. As the solution temperatures are varied continuously over a range of interest, the biomolecular thermal power is measured via the thermopile output, and then used to compute the thermodynamic parameters of the biomolecule. We present results from applying the device to DSC measurements of the unfolding of the proteins lysozyme and ribonuclease A. The enthalpy of unfolding and melting temperature of the proteins obtained are in agreement with published data.

1. Introduction

Most biochemical processes are thermally active. For example, protein folding processes, in which a protein folds into its characteristic three-dimensional structure, are typically exothermic; that is, heat is released in such processes. On the other hand, the reverse process of protein unfolding, in which the three-dimensional structure of a protein is lost under heating, absorbs heat and is hence endothermic. Measurement of heat evolved in protein folding and unfolding allows determination of the thermodynamic characteristics of these processes, which are of great importance to protein stability [1] and other biological studies. Measurement of heat, or calorimetry, is an attractive method with distinct advantages over other techniques for biomolecular characterization. Calorimetry allows direct determination of thermodynamic properties, and is universally applicable to a wide variety of biomolecules in that almost all reactions are thermally active. Additionally, calorimetric measurements occur in solution phase without requiring the biomolecule to be attached to solid surfaces. Moreover, calorimetry is label-free in that it does not require biomolecules to be labeled with a radioactive, enzymatic or fluorescent labeling groups to report molecular binding or conformational changes. Note that while calorimetric methods are generally not specific, i.e., different biochemical reactions are detected indistinguishably as heat. However, this concern is minimized by the use of purified samples, which is commonly the case for characterization of biomolecular interactions.

An important calorimetric operation mode, differential scanning calorimetry (DSC) involves measuring heat by monitoring the differential thermal activity between a biomolecular sample and a reference material in two matched calorimetric chambers whose temperatures are scanned at a specified rate over a chosen range [2,3]. Because of ubiquitous heat production or absorption in biomolecular conformational transitions such as protein folding and unfolding, DSC is widely used for characterizing such processes [4–9]. However, conventional DSC instruments in general are rather complicated in construction and low in throughput, and require large amounts of biological material [10]. These drawbacks, which have seriously hindered the application of calorimetry to biomolecular characterization, can be potentially addressed by miniaturized calorimeters enabled by microelectromechanical systems (MEMS) technology.

MEMS technology has been used to create a variety of integrated analytical devices. In particular, calorimetric sensors, thanks to their improved thermal isolation as well as reduced thermal mass and sample volume, may offer attractive advantages such as improved sensitivity and linear range, reduced power consump-

* Corresponding author at: Department of Mechanical Engineering, Columbia University, 500 W 120th Street, Room 236, New York, NY 10027, United States.
E-mail address: qlin@columbia.edu (Q. Lin).

0925-4005/$ – see front matter © 2008 Elsevier B.V. All rights reserved.
doi:10.1016/j.snb.2008.06.059

tion and shortened measurement times. When batch-fabricated in arrays, such devices may also enable high-throughput operation in which multiple samples are measured in parallel. A number of MEMS calorimetric devices have been reported in the literature. Lai et al. [11] developed a chip-based microcalorimeter for characterization of properties of polymers and other thin film materials. Jaeggi et al. [12] reported a thermoelectric AC power sensor using a polysilicon/aluminum thermopile realized by CMOS IC technology. Hagleitner et al. [13] described smart thermal sensors highly integrated with solid-state thermopiles by CMOS and micromachining technology for gas sensing. Cavicchi et al. [14] presented a MEMS calorimetric sensor with a silicon nitride diaphragm and solid-state thermopile for combustible gas detection. Barnes et al. [15] reported a bimetallic microcalorimeter with femtojoule sensitivity for use as a photothermal spectrometer. These devices, while allowing interesting calorimetric measurements, are limited to solid- or gas-phase samples, thus they are not suitable for biomolecular characterization applications that occur in liquid media.

Development and application of MEMS calorimetric devices for liquid samples are more limited. Johannessen et al. [16] and Verhaegen et al. [17] described chip-based calorimeters for measurement of catalase activity within a single mouse hepatocyte and detection of cell metabolism. Chancellor et al. [18] and Olson et al. [19] presented micromachined calorimeters that demonstrated measurement of enthalpy changes due to evaporation of water droplets. For biomoelcular measurements, Torres et al. [20] reported enthalpy arrays on large substrates to detect molecular interactions within liquid drops at the nanoliter scale, and Vivactis, NV [21] has been developing a microplate differential calorimeter for high-throughput identification and parameterization of biomolecules. In these devices, liquid samples are typically investigated in open environments, which have limitations arising from evaporation as well as a lack of well-defined sample volume for determination of specific thermodynamic properties. These limitations may be overcome by integration of MEMS calorimetric sensors with microfluidics, as has been pursued in some more recent research efforts. Lerchner et al. [22] described a miniaturized flow-through calorimeter for measuring enthalpy changes and thermal properties of catalytic reactions such as enzymatic reactions of glucose, which were also investigated by Zhang and Tadigadapa [23] with continuous-flow microfluidic devices.

We recently presented a MEMS differential thermal sensor for measuring metabolic reactions in both flow-through and flow-injection modes [24]. In this paper, the MEMS device is used to demonstrate, for the first time, DSC measurements of biomolecular interactions and conformational transitions. The device primarily consists of two calorimetric measurement chambers each based on a freestanding diaphragm, and a thin film thermopile with hot and cold junctions respectively located on the diaphragms. The chambers are fabricated from polydimethylsiloxane (PDMS) and the diaphragm from SU-8 on a silicon substrate; the use of polymeric materials allows for a low-cost device with excellent thermal isolation. DSC measurements involve filling the calorimetric chambers respectively with a biomolecular solution and a reference buffer. The device is placed in a temperature-controlled environmental chamber, so that the sample and reference temperatures can be varied precisely at a specified rate, with the differential thermal activity between the sample and reference measured by the thermopile. We demonstrate that the device allows DSC measurements of small volumes (1.2 μl) of liquid samples with a detection limit of about 30 nW and sensitivity of 1.2 nV/nW. Results from measuring the unfolding of the proteins lysozyme and ribonuclease A are shown to agree with the established properties of the proteins.

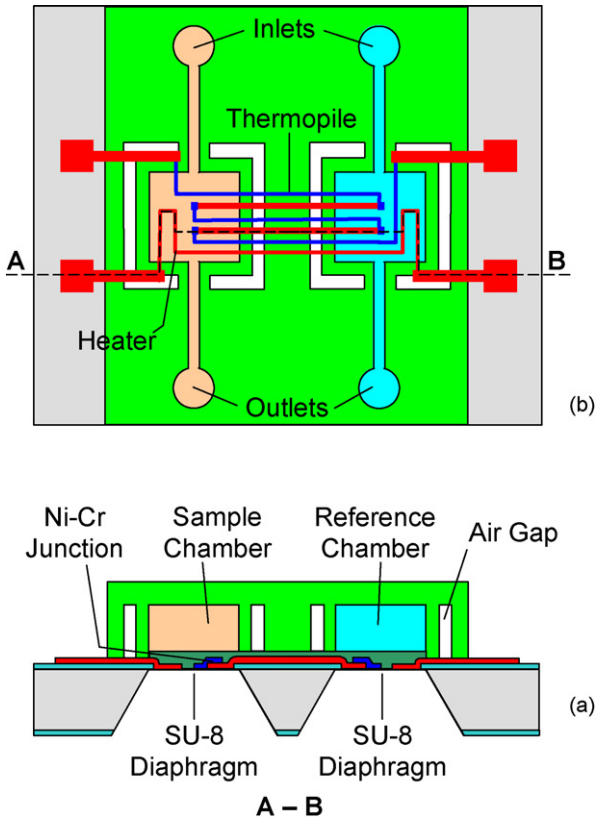

Fig. 1. Design schematic of the MEMS DSC device.

2. Design and fabrication

The MEMS DSC device monitors differences in heat capacity between a sample and a reference buffer whose temperatures are scanned at a specified rate over a continuously chosen range. The device primarily consists of a thermal sensor chip integrated with a microfluidic chip (Fig. 1). The microfluidic chip consists of two nominally identical chambers that are surrounded by air gaps and used to hold a defined volume of sample and buffer solutions for calorimetric measurements, and fluid handling microchannels that allow the solutions to be introduced into and removed from the chambers. The thermal chip includes a pair of freestanding diaphragms on which the calorimetric chambers are based, and a thin film thermopile which consists of thin films of chromium and nickel which form thermoelectric junctions. The two groups of junctions, referred to as the hot and cold junctions, are respectively located at the centers of the diaphragms. When a temperature difference exists between the hot and cold junctions, a voltage is generated over the thermopile by thermoelectric effects. A resistive heater and a temperature sensor are also incorporated on each diaphragm for device calibration and temperature control.

During device operation, the chambers are filled with a biomolecular solution and reference buffer, respectively. As the chamber temperatures are varied continuously using a thermally controlled environmental chamber (below), interactions or conformational transitions of the biomolecules either absorb or release thermal power, which can be determined in terms of the temperature difference, as measured by the thermopile, between the sample and reference.

The microfluidic chip, as well as the diaphragms on the thermal chip, is fabricated from polymers. The low thermal conductivity of the polymers (PDMS for the microfluidic chip and SU-8 for the

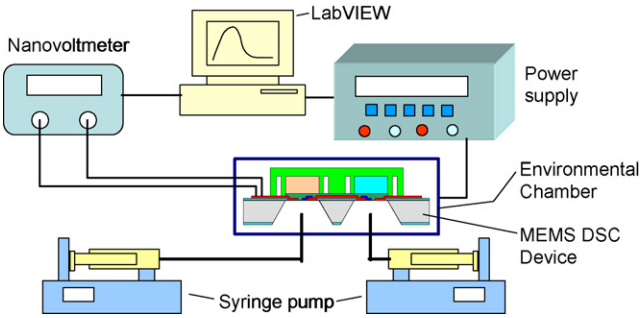

Fig. 2. Test setup for the MEMS DSC device.

diaphragms), aided by the incorporation of the air gaps surrounding the chambers, significantly improves the thermal isolation of the sample and reference solutions. Thus, a minute reaction thermal power will generate a temperature difference between the sample and reference that is sufficiently large to be detected via the thermopile voltage. Note that the freestanding diaphragms and air gaps also reduce the thermal mass of the chambers, and therefore yield an appropriate time response even in the face of the device's maximal thermal isolation.

The fabrication process has been described in detail in Ref. [24]. Briefly, chromium (0.5 μm) and nickel (0.2 μm) were deposited and patterned to form integrated resistive heaters and temperature sensors (nickel), as well as a 50-junction thermopile (nickel–chromium) on a silicon wafer that was coated with thermal oxide and etched from the backside to define the diaphragm areas. A 5-μm SU-8 thin film was then spin-coated and patterned to form the diaphragms (2 mm × 2 mm), which were later released by gas-phase XeF_2 etching for the substrate from the backside. The microfluidic chip, with the each calorimetric chamber 2000 μm × 2000 μm × 300 μm (1.2 μl) in dimension, was fabricated from PDMS using standard soft lithography methods, and checked by profilometry. The PDMS microfluidic chip was bonded to the frontside of the silicon thermal chip after oxygen plasma treatment of the bonding surfaces.

3. Experimental setup

The experimental setup as shown in Fig. 2 was used for DSC measurements. In a typical experiment, the chambers were filled with sample and reference solutions respectively using a syringe pump (KDS200, KD Scientific). A homemade external environmental chamber served as a thermal shield to minimize fluctuations in ambient conditions, and provided closed-loop temperature control for temperature scanning of the device. As such, the sample and solution temperatures were scanned at a constant rate and the thermopile output voltage was obtained. A nanovoltmeter (34420A, Agilent) was used to measure the thermopile output voltage. The on-chip heaters were connected to a universal power supply (E3631A, Agilent) to apply a known amount of Joule heating power to the chambers during device calibration. A PC with a LabVIEW (National Instruments) program was used to automate the experiment.

4. Determination of thermodynamic parameters

As the sample and reference solution temperatures are scanned at a constant rate over a given range, thermal power, denoted P_s and P_r, respectively for the sample and reference, is evolved in the solutions. This causes the sample temperature (T_s) and reference temperature (T_r) to differ slightly. When the device's thermal time constant is small compared with the time scale of biomolecular interaction to be measured, it is reasonable to assume that the heat transfer process in the device is in steady-state. Then, the temperature difference, $\Delta T = T_s - T_r$, is related to the power difference, $\Delta P = P_s - P_r$, by a linear relationship: $\Delta T = R\Delta P$. Meanwhile, the temperature difference is also proportional to the voltage, ΔU, on the thermopile (i.e., the device output) according to the relationship $\Delta U = S\Delta T$, where S is the Seebeck coefficient of the thermopile. Thus, from the device output, one can obtain the power difference between the sample and reference by

$$\Delta U = K\Delta P \tag{1}$$

where $K = SR$ is the device responsivity. Note that the baseline, which is the device output when both the sample and reference chambers are filled with the same buffer solution and their temperatures scanned over the chosen range, is in general nonzero because of device fabrication limitations. Therefore, the device output ΔU should include corrections by subtraction of this baseline.

The effects of the biomolecular interaction are manifested by a change of heat capacity of the sample solution. Let C_s and C_r be the effective heat capacities of the sample and reference chambers and the solutions contained therein, respectively. Then, the effective heat capacity difference, $\Delta C = C_s - C_r$, can be determined from the thermal power difference by

$$\Delta C = \frac{\Delta P}{\dot{T}} \tag{2}$$

where $\dot{T}$ is the rate at which the nominally equal temperatures of the solutions, T, is scanned. As T is varied over a range of interest, ΔP, and hence ΔC, are obtained as a function of T.

The heat capacity difference also equals the difference in heat capacities of the biomolecule and the buffer solution it displaces out of the sample chamber. That is,

$$\Delta C = c_{mol} m_{mol} - c_{solv}\,\Delta m_{solv} \tag{3}$$

where c_{mol} and c_{solv} are the partial specific heat capacities of the biomolecule and solvent, respectively. Here, m_{mol} is the mass of the biomolecule in the sample chamber, which can be obtained as the product of the biomolecule concentration and chamber volume. Additionally, Δm_{solv} is the mass of the displaced solvent, which is related to the biomolecule mass by

$$\Delta m_{solv} = m_{mol}\left(\frac{v_{mol}}{v_{solv}}\right) \tag{4}$$

where υ_{mol} and υ_{solv} are the partial specific volumes of biomolecules and the solvent, respectively. Substituting Eq. (4) into Eq. (3), and solving the resulting equation yield

$$c_{mol} = c_{solv}\left(\frac{v_{mol}}{v_{solv}}\right) + \left(\frac{\Delta C}{m_{mol}}\right) \tag{5}$$

In general, all quantities in this equation are temperature-dependent. As a first approximation, however, one may ignore the temperature dependence of the biomolecule mass m_{mol} and the specific volume ratio $\upsilon_{mol}/\upsilon_{solv}$, which can be evaluated from published data at room temperature. Then, this equation allows for the determination of the biomolecule's heat capacity c_{mol}, as a function of temperature, in terms of the experimentally determined effective heat capacity difference ΔC and well established temperature-dependent solvent specific heat c_{solv}.

Integrating the biomolecular heat capacity with respect to temperature then allows for further determination of the specific enthalpy change associated with the biomolecular interaction:

$$\Delta H(T) = \int_{T_1}^{T} \Delta c_{mol}(T)\,dT \tag{6}$$

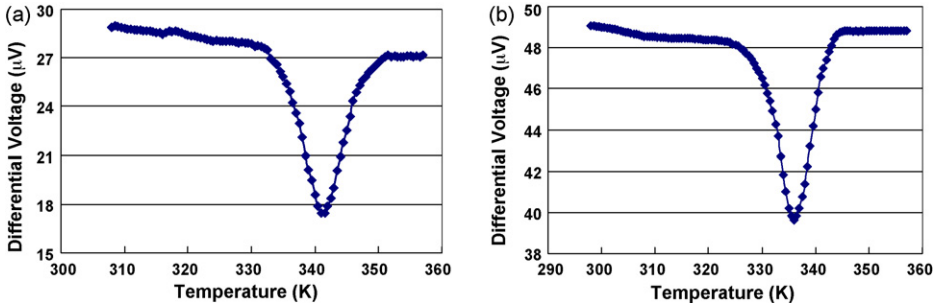

Fig. 3. Device output as a function of temperature during unfolding of the proteins: (a) lysozyme and (b) RNase A.

where the temperature range over which the solution temperatures are scanned is defined by the extreme temperatures T_1 and T_2. As the temperature T is varied over this range, the enthalpy change is also obtained as a function of T. In particular, $\Delta H_{tot} = \Delta H(T_2)$ is the total enthalpy change of the biomolecule over the temperature range. Moreover, in the case of conformational transitions between a biomolecule's native and denatured states as corresponding to the temperatures T_1 and T_2, the assumption of a two-state model allows the determination of the melting temperature of the biomolecule, T_m, as the midpoint between the two states [25]:

$$\Delta H(T_m) = \frac{\Delta H_{tot}}{2} \tag{7}$$

5. Experimental results

We first performed the characterization of the thermopile and the calibration of the device for differential measurements, the details of which have been described in Ref. [24]. It was found that the thermopile voltage was highly linear with the temperature difference between the thermopile's hot and cold junctions. The total Seebeck coefficient, or thermopile voltage per unit temperature difference, was found to be $S = 1.85$ mV/K, in agreement with published data [26].

To calibrate the device for DSC measurements, the calorimetric chambers were both filled with phosphate buffered saline (PBS) buffer (pH 6.8). The microheater in the sample chamber was used to impart a known, constant Joule heating power to the solution therein. With the reference chamber remaining unheated, the steady-state thermopile output was measured, allowing for determination of the power difference between the calorimetric chambers as a highly linear function of temperature. Accordingly, the device responsivity was determined to be $K = 1.2$ nV/nW (Eq. (1)). This responsivity also allowed us to determine, from the measured thermopile voltage noise, the baseline noise in the power difference to be approximately 30 nW between the chambers when they were kept at a constant temperature of 300 K.

With the calorimetric chambers filled with PBS buffer, we also tested the device's time-resolved transient behavior in response to a unit-step thermal power difference. This allowed the determination of the thermal time constant of the device to be approximately 0.6 s. As biomolecular transitions typically occur at much longer time scales (e.g., several minutes), the device's thermal response is generally sufficiently fast for DSC measurements.

The calibrated MEMS DSC device was applied to measuring thermally induced protein unfolding, a phenomenon in which a protein loses its three-dimensional structure and hence its function. In the DSC measurements, the sample chamber was filled with a protein solution (prepared in PBS buffer), while the reference chamber was filled with PBS buffer in the absence of the protein. The sample and reference solutions were both degassed prior to the filling process. The solution temperatures were scanned at a constant rate using the environmental chamber (Fig. 2) and the thermopile output voltage was obtained.

We have demonstrated MEMS DSC measurements by the unfolding of the proteins lysozyme (chicken egg white, Sigma–Aldrich) and ribonuclease A (RNase A, bovine pancreas, Fluka), whose thermodynamic characteristics are well known. The protein solutions were prepared in PBS buffer at concentrations of 20 mg/ml (lysozyme) and 18 mg/ml (RNase A), respectively. The temperature scanning rate was 5 K/min. The measured device output, corrected by baseline subtraction, is shown in Fig. 3. Using the device responsivity given above, the power difference between the chambers was obtained from Eq. (1). Accordingly, the effective heat capacity difference was determined from Eq. (2) (Fig. 4). It can be observed from Figs. 3 and 4 that the thermopile output exhibits a deep valley and the effective heat capacity difference a sharp peak, reflecting the endothermic nature of the protein unfolding processes.

The effective heat capacity difference allows us to obtain the partial specific heats of the proteins according to Eq. (5). For this purpose, the specific volumes of lysozyme (molecular weight: 14.3 kDa) and RNase A (molecular weight: 13.7 kDa) are taken to be 0.742 and 0.707 ml/g, respectively [9]. The PBS buffer is assumed to

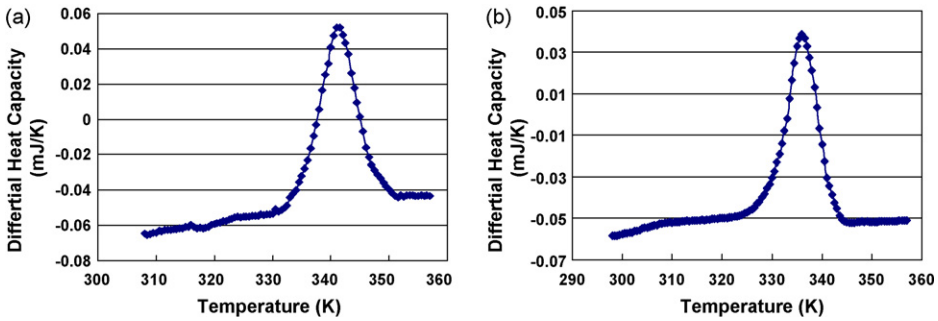

Fig. 4. Heat capacity difference as a function of temperature during unfolding of the proteins: (a) lysozyme and (b) RNase A.

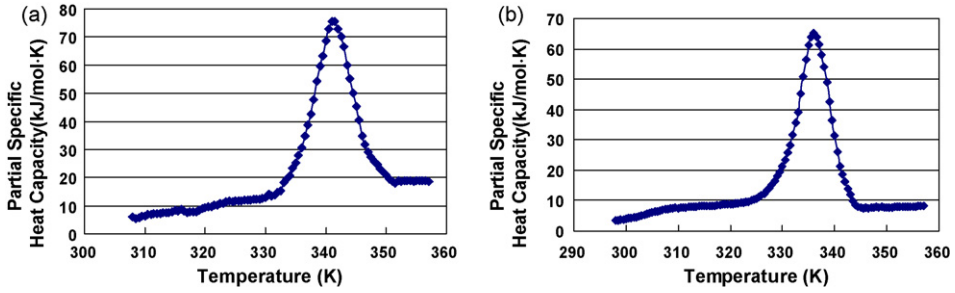

Fig. 5. Partial specific heat capacities of: (a) lysozyme and (b) RNase A during unfolding of the proteins.

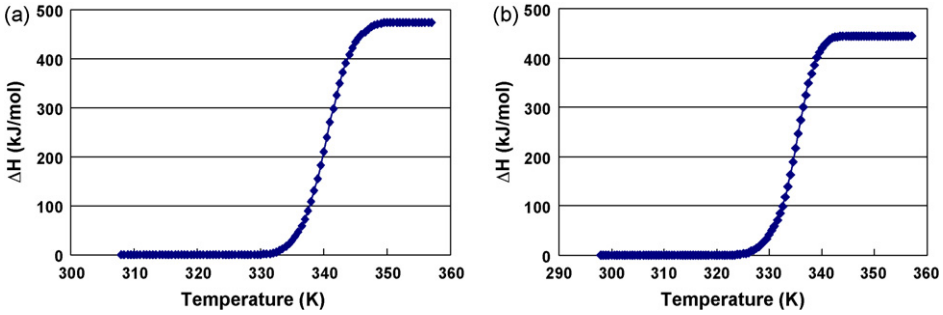

Fig. 6. Enthalpy change and melting temperature for unfolding of the proteins: (a) lysozyme and (b) RNase A.

have a specific volume of 1 ml/g with specific heat c_{solv} = 4.186 J/g K. The volume of each chamber is given the nominal value of 1.2 μl. The partial specific heats for the proteins computed from the effective heat capacity difference (Fig. 4) are shown in Fig. 5. It can be seen that similar to the effective heat capacity, the partial specific heat exhibits a strong temperature dependency and a baseline shift between the native and denatured states. In particular, the specific heats of the proteins increase sharply during unfolding, characteristic of an endothermic process.

The specific enthalpy change of the proteins during the unfolding process can be obtained by integrating the partial specific heat according to Eq. (6). This can be carried out by numerical integration, and the results are shown in Fig. 6. The shape of the enthalpy transition curves is consistent with established knowledge for the proteins, whose unfolding can be well represented by a two-state model [1,25]. The enthalpy change of unfolding, or the total enthalpy change between the native and denatured states, is determined from these curves to be 474 kJ/mol for lysozyme and 444 kJ/mol for RNase A. These compare favorably with published data (e.g., 427–481 kJ/mol for lysozyme [1,8,25,27] and 372–481 kJ/mol for RNase A [1,28]). Additionally, according to Eq. (7), the melting temperature can be determined for the proteins from the enthalpy transition curves to be 340.5 K (67.3 °C) for lysozyme and 335.1 K (61.9 °C) for RNase A, respectively. These are also consistent with published data (e.g., 55–74.7 °C for lysozyme [1,8,25,27] and 59–64 °C for RNase A [1,28]).

6. Conclusion

This paper presents the first demonstration of differential scanning calorimetry (DSC) using a MEMS device, aiming to address label-free, solution-based characterization of biomolecular interactions and conformational transitions with much reduced sample consumption. The device consists of a pair of polydimethylsiloxane (PDMS) calorimetric microchambers and fluid handling microchannels integrated with a thermal sensor chip featuring freestanding SU-8 diaphragms. The chambers are each 1.2 μl in volume and based upon a diaphragm. A nickel–chromium thermopile, and nickel heaters and temperature sensors, are integrated on the diaphragms to allow temperature measurement and control. The low thermal conductivities of the PDMS and SU-8 polymers, aided by the use of air gaps surrounding the chambers, offer excellent thermal isolation. During DSC measurements, the chambers are filled with a biomolecular solution and reference buffer, respectively. As the chamber temperatures are varied continuously by an environmental chamber in which the device is placed, biomolecular interactions or conformational transitions either absorb or release thermal power, which can be determined in terms of the temperature difference, as measured by the thermopile, between the sample and reference. With a thermal power noise level of about 30 nW, we have demonstrated DSC measurements of the unfolding of proteins lysozyme and ribonuclease A (RNase A) at concentrations of 20 and 18 mg/ml, respectively. Using the measurement data, we have determined that the enthalpy of unfolding is 474 kJ/mol for lysozyme and 444 kJ/mol for RNase A, respectively. Additionally, the melting temperature has been determined to be 67.3 °C for lysozyme and 61.9 °C for RNase A, respectively. These thermodynamic parameters are found to be in good agreement with published data. With the potential of MEMS-based DSC measurements demonstrated in this paper, design improvements in the future, such as further enhanced thermal isolation and more sensitive thermoelectric sensing, are expected to allow such measurements to be performed at more dilute biomolecule concentrations.

Acknowledgments

The authors gratefully acknowledge the financial support from Biomolecular Interaction Technologies Center, University of New Hampshire, and National Science Foundation (Grant # DBI-0650020). We also appreciate insightful discussions with Professors Jonathan B. Chaires at the University of Louisville and Edwin A. Lewis at the University of Northern Arizona.

References

[1] A.D. Robertson, K.P. Murphy, Protein structure and the energetics of protein stability, Chemical Reviews 97 (1997) 1251–1267.
[2] G.W.H. Hohne, W.F. Hemminger, H.-J. Flammersheim, Differential Scanning Calorimetry, 2nd ed., Berlin, Springer, 2004.
[3] T. Hatakeyama, F.X. Quinn, Thermal Analysis: Fundamentals and Applications to Polymer Science, 2nd ed., Wiley, New York, 1999.
[4] G.P. Privalov, P.L. Privalov, Problems and prospects in microcalorimetry of biological macromolecules, Energetics of Biological Macromolecules 323 (2000) 31–62.
[5] J.F. Brandts, L.-N. Lin, Study of strong to ultratight protein interactions using differential scanning calorimetry, Biochemistry 29 (1990) 6927–6940.
[6] V.V. Plotnikov, J.M. Brandts, L.-N. Lin, J.F. Brandts, A new ultrasensitive scanning calorimeter, Analytical Biochemistry 250 (1997) 237–244.
[7] E. Freire, G. Privalov, P. Privalov, V. Kavina, Device and methods for the heat of reaction resulting from mixture of a plurality of reagents, US Patent No. 5707149 (1998).
[8] G. Privalov, V. Kavina, E. Freire, P.L. Privalov, Precise scanning calorimeter for studying thermal properties of biological macromolecules in dilute solution, Analytical Biochemistry 232 (1995) 79–85.
[9] P. Privalov, S. Potekhin, Scanning microcalorimetry in studying temperature-induced changes in proteins, Methods in Enzymology 131 (1986) 4–51.
[10] MicroCal, LLC, Use of isothermal titration calorimetry to measure enzyme kinetics parameters, www.microcalorimetry.com.
[11] S.L. Lai, G. Ramanath, L.H. Allen, High-speed scanning microcalorimetry with monolayer sensitivity, Applied Physics Letters 67 (1995) 1229–1231.
[12] D. Jaeggi, H. Baltes, D. Moser, Thermoelectric AC power sensor by CMOS technology, IEEE Electron Device Letters 13 (1992) 366–368.
[13] C. Hagleitner, A. Hierlemann, D. Lange, A. Kummer, N. Kerness, O. Brand, H. Baltes, Smart single-chip gas sensor microsystem, Nature 414 (2001) 293–296.
[14] R.E. Cavicchi, G.E. Poirier, N.H. Tea, M. Afridi, D. Berning, A. Hefner, I. Suehle, M. Gaitan, S. Semancik, C. Montgomery, Micro-differential scanning calorimeter for combustible gas sensing, Sensors and Actuators B 97 (2004) 22–30.
[15] J.R. Barnes, R.J. Stephenson, C.N. Woodburn, S.J. O'Shea, M.E. Wellan, T. Rayment, J.K. Gimzewski, C. Gerber, A Femtojoule calorimeter using micromechanical sensors, Review of Scientific Instruments 65 (1994) 3793–3798.
[16] E.A. Johannessen, J.M.R. Weaver, P.H. Cobboid, J.M. Cooper, Heat conduction nanocalorimeter for pl-scale single cell measurement, Applied Physics Letters 80 (2002) 2029–2031.
[17] K. Verhaegen, K. Baert, J. Simaels, W. van Dressche, A high-throughput silicon microphysiometer, Sensors and Actuators A 82 (2000) 186–190.
[18] E.B. Chancellor, J.P. Wikswo, F. Baudenbacher, M. Radparvar, D. Osterman, Heat conduction calorimeter for massively parallel high throughput measurements with picoliter sample volumes, Applied Physics Letters 85 (2004) 2408–2411.
[19] E.A. Olson, M.Y. Efremov, A.T. Kwan, S. Lai, V. Petrova, F. Schiettekatte, J.T. Warren, M. Zhang, L.H. Allen, Scanning calorimeter for nanoliter-scale liquid samples, Applied Physics Letters 77 (2000) 2671–2673.
[20] F.E. Torres, P. Kuhnt, D.D. Bruyker, A.G. Bell, M.V. Wolkin, E. Peeters, J.R. Williamson, G.B. Anderson, G.P. Schmitz, M.I. Recht, S. Schweizer, L.G. Scott, J.H. Ho, S.A. Elrod, P.G. Schultz, R.A. Lerner, R.H. Bruce, Enthalpy arrays, Proceedings of the National Academy of Sciences of USA 101 (2004) 9517–9522.
[21] Vivactis, NV, www.vivactis.com.
[22] A.W.J. Lerchner, G. Wolf, V. Baier, E. Kessler, M. Nietzsch, M. Krugel, A new microfluid chip calorimeter for biochemical applications, Thermochimica Acta 445 (2006) 144–150.
[23] Y. Zhang, S. Tadigadapa, Calorimetric biosensor with integrated microfluidic channels, Biosensors and Bioelectronics 19 (2004) 1733–1743.
[24] L. Wang, D. Sipe, Q. Lin, A MEMS thermal biosensor for metabolic monitoring applications, Journal of Microelectromechanical Systems 17 (2008) 318–327.
[25] H.-J. Hinz, F.P. Schwarz, Measurement and analysis of results obtained on biological substances with D.S.C., Journal of Chemical Thermodynamics 33 (2001) 1511–1525.
[26] D.M. Rowe, CRC Handbook of Thermoelectrics, 1st ed., CRC Press, Boca Raton FL, 1995.
[27] A. Bhambhani, C.V. Kumar, Enzyme-inorganic nanoporous materials: differential scanning calorimetric studies and protein stability, Microporous and Mesoporous Materials 109 (2008) 223–232.
[28] F.P. Schwarz, Interaction of cytidine 3′-monophosphate and uridine 3′-monophosphate with ribonuclease-A at the denaturation temperature, Biochemistry 27 (1988) 8429–8436.

Biographies

Li Wang received his PhD in Mechanical Engineering from Carnegie Mellon University in 2007. Previously, he received the B.S. (1999) and M.S. (2002) degrees in Mechanical Engineering from Tsinghua University, Beijing, China. His research interests include miniaturized devices with integrated microfluidics for biomedical applications.

Bin Wang received his B.S. (2003) in Mechanical Engineering from the University of Science and Technology of China, and M.S. (2006) in Microelectronics and Solid-State Electronics from Shanghai Institute of Microsystem and Information Technology, Chinese Academy of Sciences. He is currently a PhD candidate in the Department of Mechanical Engineering at Columbia University. His research interests include biomedical applications of microelectromechanical systems (BioMEMS).

Qiao Lin received the PhD degree in Mechanical Engineering from the California Institute of Technology in 1998 with thesis research in robotics. Dr. Lin conducted postdoctoral research in microelectromechanical systems (MEMS) at the Caltech Micromachining Laboratory from 1998 to 2000, and was an Assistant Professor of Mechanical Engineering at Carnegie Mellon University from 2000 to 2005. He has been an Associate Professor of Mechanical Engineering at Columbia University since 2005. His research interests are in designing and creating integrated micro/nanosystems, in particular MEMS and microfluidic systems, for biomedical applications.